IEEE Pub. No. 81CH1715-2 NPS

9th Symposium on Engineering Problems of Fusion Research

Palmer House
Chicago, Illinois
October 26-29, 1981

PROCEEDINGS

Volume I

Editor
Chan K. Choi
University of Illinois at Urbana-Champaign

Meeting Cosponsors

University of Illinois, Fusion Studies Laboratory
Institute of Electrical and Electronics Engineers
Nuclear and Plasma Sciences Society
Department of Energy, Office of Fusion Energy
American Nuclear Society
Argonne National Laboratory
Electric Power Research Institute

Available from:
IEEE Service Center
Single Publication Sales Dept.
445 Hoes Lane
Piscataway, N.J. 08854

Printed in USA

OVERVIEW OF INTOR NUCLEAR SYSTEMS*

Mohamed A. Abdou

Fusion Power Program
Argonne National Laboratory
Argonne, Illinois 60439

Summary

A serious effort was devoted in the Phase-I study for INTOR to identifying critical issues and developing credible design concepts for the nuclear systems. Erosion by charge-exchange neutrals and effects of plasma disruption are key issues for the first wall. A melt layer is predicted to develop in a bare stainless steel wall under plasma disruptions. Graphite tiles will not melt but they introduce serious uncertainties into the design. A partial tritium-producing blanket will be installed on INTOR to reduce the cost of externally supplied tritium. The key issue in the solid breeder blanket concept relates to the effect of radiation on tritium inventory in the blanket. The design strategy for the divertor collector plate focused on separating the surface and high heat flux problems and on utilizing a novel mechanical design concept for attaching tungsten tiles to a stainless steel (or copper) heat sink.

Introduction

A number of papers[1-3] in this conference provide an overview of the INTOR design and a description of physics and mechanical engineering features. This paper is devoted to presenting a summary of the work in selected areas of the nuclear systems. The focus is on providing an overview of the key issues and the design for the first wall, breeding blanket, and divertor. The details of the work are presented in Refs. 4-8.

First Wall System

A conceptual design of a first-wall system that will survive the total reactor life has been developed for INTOR. The first-wall system consists of (1) an outboard region that serves as the major fraction of the plasma chamber surface and receives particle and radiation heat fluxes from the plasma and radiative heating from the divertor; (2) an inboard region that receives radiative and particle fluxes during the plasma burn and the major fraction of the plasma energy during a disruption; (3) a limiter region on the outboard wall that serves to form the plasma edge during the early part of startup; (4) a beam-shine-through region on the inboard wall that receives shine-through of the neutral beams at the beginning of neutral injection; and (4) a region on the outboard wall that receives enhanced particle fluxes caused by ripple effects during the late stages of neutral injection. Figure 1 is a poloidal view of the reactor showing the location of the various first-wall regions. Table 1 summarizes the operating parameters for the first-wall system.

The reference concept for all first-wall regions is a water-cooled stainless steel panel (see Fig. 1). The wall thickness of the special regions, e.g., the limiter and inboard regions, is increased to allow for enchanced erosion caused by the preferential heat or particle fluxes. The 20% cold-worked Type 316 stainless steel, which is selected as the structural material, provides adequate radiation damage resistance

*Work supported by U. S. Department of Energy.

Table 1. INTOR First-Wall Operating Parameters

First Wall	
Total plasma chamber area, m^2	380
Average neutron wall loading, MW/m^2	1.3
Radiative power to first wall, MW	40
Charge-exchange	
Power, MW	4
Current (50% D, 50% T), s^{-1}	1.3×10^{23}
Flux, $m^2 s^{-1}$	3.3×10^{20}
Energy, eV	200
Cycle time (Stage I/Stage II & III), s	145/245
Burn time (Stage I/Stage II & III), s	100/200
Total disruption energy, MJ	220
Disruption time, ms	20
Operating life,	15
Total average neutron flux, n/m^2	6.8×10^{26}
Integral neutron wall load, $MW\text{-}y/m^2$	6.5
Total number shots	7.1×10^5
Total number disruptions	1080
Outboard Wall	
Area, m^2	266
Surface heat flux, W/cm^2	
From plasma	11.6
From divertor	3.4
Total	15
Average nuclear heating, W/cm^3	15
Limiter	
(Outboard wall at R ~ 6 m - Upper and Lower.)	
Width, m	1
Area (each), m^2	38
Total ion flux, s^{-1}	3×10^{23}
Total heat flux, MW	10
Total ion heat flux, MW	5
Heat flux density, MW/m^2	0.3
Peaking factor	1.5
Typical particle energy, eV	100
Duration, s	4
Period, s	t = 0-4
Ripple Armor	
(Outboard wall at R = 6 m - Upper and Lower.) (Does not coincide with the limiter.)	
Area, m^2	26
Heat flux (ripple = ±0.5%), MW/m^2	0.4
Peaking factor	2
Particle energy (D), keV	120
Period, s	t = 8-10
Inboard Wall	
Area, m^2	114
Surface heat flux, W/cm^2	11.6
Average nuclear heating, W/cm^3	10
Peak disruption energy density, J/cm^2	289
Beam-Shine-Through Region (Inboard Wall)	
Total power (5% of injected), MW	4
Particle energy, keV	175
Duration, s	2
Period, s	t = 4-6
Area, m^2	4
Heat flux, MW/m^2	1

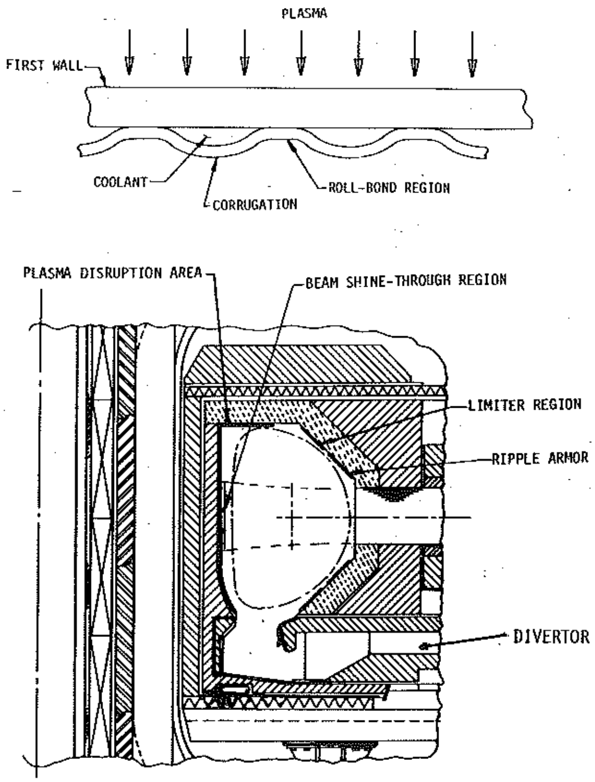

Fig. 1. First-wall cross section (top) and first-wall configuration (bottom).

for full life and allowable design stress intensity sufficient to meet code specifications for the reference conditions. The thin corrugated coolant channels in the panel-type construction selected for the first wall tend to minimize bending stresses and provide longer lifetime than tubes. The outboard wall is integral with the blanket and serves as the containment for the neutron multiplier.

The erosion rates and thickness requirements for the various regions of the first-wall panel have been evaluated. The physical sputtering erosion rates are based on effective sputtering yields of 0.020 atoms per particle at 200 eV and 0.0072 atoms per particle at 100 eV for the particle composition given in Table 1. The calculated vaporization erosion caused by a plasma disruption is 8×10^{-4} mm per disruption fo[r] 289-J/cm^2 energy density deposited in 20 ms. An uncertainty factor of two is used to obtain the de[sign] erosion allowance. It is assumed that the melt la[yer] formed during a disruption does not erode.

Table 2 is a summary of the lifetime analysis [of] the first-wall system. For the wall thickness requirements necessary to allow for these predicted [ero]sion rates, all regions meet the design temperatur[e,] stress and fatigue criteria for full-life operatio[n] under the reference conditions. The major uncerta[inty] in this design concept relates to the stability of [the] melt layer formed during a disruption. A grooved [in]board wall concept would accommodate erosion of up [to] 10% of the melt layer (~0.14 mm/disruption). Furt[her] research and development are required to confirm t[he] stability of the melt region during a disruption.

Tritrium Producing Blanket

A partial tritium breeding blanket will be installed on INTOR to reduce the cost of externally supplied tritium. Liquid (lead-lithium-bismuth) a[nd] solid breeders were considered. The technology fo[r] tritium extraction from a liquid breeder is relati[vely] well understood, but the blanket design is rather [com]plicated, relative to a nonbreeding blanket. The blanket design for a solid breeder is much less co[m]plicated, but the uncertainty about radiation effe[cts] upon tritium release is a major concern. Research programs are currently underway which should resol[ve] this uncertainty within the next year or so. The solid breeder was selected for INTOR based on the lower risk of the engineering design and the fact [that] the present uncertainty about tritium release will [be] resolved in the near future.

The breeding blanket in INTOR uses the top a[nd] outboard portion of the 12 removable blanket/shiel[d] sectors. To permit a blanket design which is easi[ly] adapted to the varying width of the top region and the changes in neutron wall loading with distance [from] the midplane, two key features were adopted: (1) [a] modular approach, by which the blanket is divided poloidally into a number of discrete segments; (2) coolant flow through the module across the full se[ctor] width, in the toroidal direction

An isometric breakout view of a typical breed[ing] blanket module is shown in Fig. 2. Design and ope[rat]ing parameters for the blanket are given in Table

Table 2. Summary of Lifetime Analysis

Region	Total Thickness (mm)	Maximum Erosion (mm)	Maximum[a] Temp. (°C)	Maximum[b] Stress (MPa)	Fatigue Life, Cycles: No Erosion	Fatigue Life, Cycles: W/Erosion[c]
Outboard wall	11.7	8.7[d]	260	360	3×10^6	$>10^7$
Ripple region	11.7	8.7[d]	297	400	1×10^6	$>10^7$
Limiter region	12.8	9.8[d]	280	410	8×10^5	$>10^7$
Inboard wall	13.5	10.5[e]	275	408	9×10^5	$>10^7$
Beam-shine-through region	13.5	10.5[e]	332	495	2×10^5	$>10^7$

[a]Maximum specified temperature = 350°C.

[b]Maximum allowable stress = 650 MPa plasma side, 765 coolant side (cold-worked material).

[c]Assumes erosion rate one-half of predicted rate for conservative design.

[d]Physical sputtering.

[e]Physical sputtering plus vaporization.

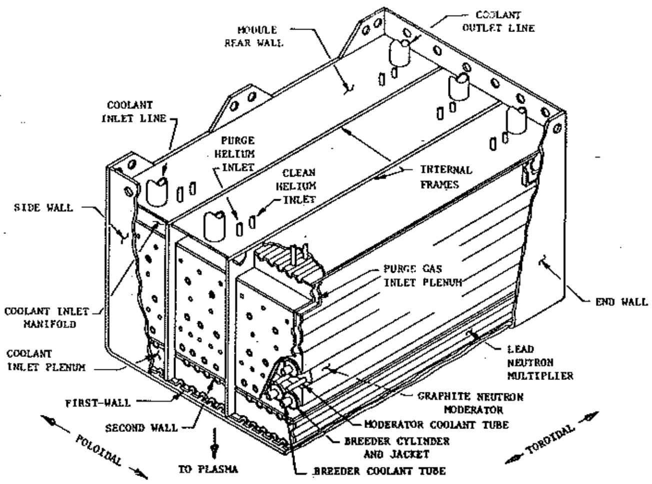

Fig. 2. Reference tritium- producing blanket design.

Table 3. Summary of Rference Design Parameters for Tritium-Producing Blanket

Neutron multiplier	
Material	Pb
Maximum temperature, °C	290
Melting point, °C	327
Thickness, m	0.05
Theoretical density, g/cm^3	11.34
Effective density, %	100
Second wall	
Form	Corrugated panel
Structural materials	316 SS
Max. structural temperature, °C	<150
Total structual thickness, mm	2.5
Coolant	H_2O
Coolant outlet temperature, °C	100
Coolant inlet temperature, °C	50
Coolant nominal pressure, MPa	0.7
Region thickness, mm	6.0
Breeding region	
Structural material	316 SS
Max. structural temperature, °C	<150
Breeder material	Li_2SiO_3
Theoretical density, g/cm^3	2.53
Effective density, %	70
Grain size, 10^{-6} m	<1
Breeder max./min. temperature, °C	600/400
Neutron moderator material	Graphite
Effective density, g/cm^3	1.9
Moderator zone gas	He (0.10 MPa)
Region thickness, m	0.43
Coolant	H_2O
Coolant outlet temperature, °C	100
Coolant inlet temperature, °C	50
Coolant nominal pressure, MPa	0.7
Tritium processing fluid	He (0.10 MPa)

The blanket design features a solid lithium compound breeder, Li_2SiO_3, with lithium enriched to 30% of ^6Li. The solid breeder is fabricated at 70% of theoretical density. Adequate tritium breeding is achieved by using lead as a neutron multiplier. Graphite neutron moderator is used in the breeding zone to minimize solid breeder inventory. Tritium is removed from the breeder by a gaseous helium purge stream. Breeder minimum and maximum temperatures during operation are 400°C and 600°C. This temperature range and the 70% density facilitate tritium diffusion from the breeder. The low lithium inventory helps reduce the part of tritium inventory related to solubility. Pressurized light water (H_2O) is used to cool all parts of the blanket module. Type 316 stainless steel is used for all structural and pressure-carrying components.

The first-wall panel serves as the plasma-side containment for the neutron multiplier, and its cooling system removes part of the lead neutron multiplier's volumetric heat. The containment at the back face of the multiplier is also an actively cooled corrugated panel (second wall), which removes the remainder of the multiplier's volumetric heat. The first wall and second wall are joined by intercostals which extend through the 5-cm thick multiplier, thus combining the two panels structurally into a relatively deep two-cap beam. The panels, the module side walls, and end walls form a pressure boundary around the multiplier. Low-pressure helium in this zone provides good thermal conductance at the multiplier/coolant panel interfaces. Maximum multiplier temperature is predicted to be 290°C, well below the 327°C melting point of lead.

The lithium silicate behind the neutron multiplier is formed in cylinders around single-wall stainless steel coolant tubes. There are three separate rows, or banks, of breeder cylinder/coolant tube assemblies, which are separated radially within the breeding zone. The graphite neutron moderator is located between banks and between the third bank and the back wall of the module. Separate, small-diameter coolant tubes cool the moderator.

A thin metal jacket surrounds each breeder cylinder. This jacket provides a pressure boundary between the helium purge gas which flows through the breeder cylinder, and the "clean" helium which fills the remainder of the breeding zone and the multiplier zone. The clean helium provides good thermal conductance between the moderator and the jackets. Jacket temperature during reactor operation is relatively low to maintain a low permeability barrier against tritium migration from the purge gas into the graphite.

Coolant inlet and outlet temperatures are 50°C and 100°C. The coolant is pressurized to 0.7 MPa (100 psi). The moderator coolant tubes and breeder coolant tubes all connect to coolant inlet and outlet plenums located at the module sides (in the poloidal plane). These plenums also connect to the first wall and second wall. At the rear of the blanket the plenums are widened, to serve as a manifold region. These manifolds are connected to large-diameter coolant lines which extend through the bulk shield behind the module.

Helium purge gas inlet and outlet plenums are located between the coolant plenums and the breeding zone. The purge gas flows inside the jackets through several narrow gaps which extend radially through the breeder cylinder. A low partial pressure of oxygen in the 1 atm pressure purge helium reacts with the free tritium at the surface of the breeder particles to form T_2O and HTO, which enter the purge gas stream. The purge gas plenums are connected to small diameter lines which pass through the bulk shield.

The tritium inventory in the blanket should be about 1 kg, based upon present knowledge of tritium release data. Radiation effects upon tritium release could possibly result in a significantly larger inventory, but these effects are uncertain at present.

Divertor Collector Plate

The impurity control system in INTOR is a single-null poloidal divertor located at the bottom of Fig. 1. The purpose of the divertor is to collect the ionized particles that have escaped from the plasma along with the sputtered particles from the first wall. The divertor effort for INTOR considered the important aspects of physics, magnetics, engineering, and maintenance. A summary of the operating conditions is shown in Table 4. The total power to the divertor is 80 MW, which is equally divided between the inner and outer channels. A total of 70 MW of that power impinges directly on the divertor collector plates resulting in high surface heat and particle fluxes, in addition to the usual neutron flux. The inner plate is placed at an angle of 30 deg and the outer plate is placed at an angle of 14.5 deg with respect to the separatrix. The angular placement reduces the peak surface heat flux to 2 MW/m^2 and the peak particle flux to $1.5 \times 10^{22}/m^2$-s.

Table 4. Divertor Operating Conditions

Total power to divertor, MW	80
Ion power to divertor plates, MW	35
Electron power to divertor plates, MW	35
Ion flux to divertor plates, s^{-1}	5.5×10^{23}
Average energy of ions, eV	400
Composition of ions, %	
T 47	
D 47	
He	5
C 0.5	
O 0.5	
Neutral gas density at front of divertor plates, m^{-3}	10^{19}
Peak power flux to divertor plates normal to separatrix, MW/m^2	
Outboard	8
Inboard	4
Peak ion flux to divertor plates perpendicular to separatrix, m^2-s^{-1}	
Outboard	6×10^{22}
Inboard	3×10^{22}
Inclination of divertor plate to separatrix, deg	
Outboard	14.5
Inboard	30
Total power to throat and channel, MW	10
Charge-exchange neutrals, MW	5
Radiation, MW	5
Total neutral flux, s^{-1}	1.6×10^{23}
Average energy of neutrals, eV	200
Peaking factor of flux	2
Area on which the neutrals impinge,[a] m^2	33

[a]Five strips of length 0.2 m each, four of them being adjacent to the ends of the divertor plates and the fifth on the wall facing the outside divertor plate.

The severe operating conditions make the divertor collector plate the most heavily damaged torus component. The key design issues for the collector plate are: (a) sputtering loss of material; (b) thermal stress and fatigue; radiation damage, e.g. swelling and embrittlement; (d) redeposition of eroded material from the first wall and collector plate; (e) electromagnetic forces induced in the collector plate during plasma disruptions; (f) tritium permeation into the col[illegible] plate coolant; and (g) maintainability of the col[illegible] plate which requires periodic replacement.

During Phase-I, several potential design con[illegible] for a divertor collector plate were analyzed, and designs were then selected and analyzed in furthe[illegible] detail. In both designs, the problems of sputte[illegible] separated from the problems of cooling and struct[illegible] support. The designs employ a low sputtering pr[illegible] plate that is attached to a heat sink composed of standard structural alloy. The main difference [illegible] the designs is in the method of attachment of the [illegible]tection plate to the heat sink. One design empl[illegible] braze to produce a high thermal conductance path strong bond to the heat sink (high conductance de[illegible] The other designs employs mechanical attachments produce a low thermal conductance path and a weak to the heat sink (low conductance design). The [illegible] designs are compared in Fig. 3.

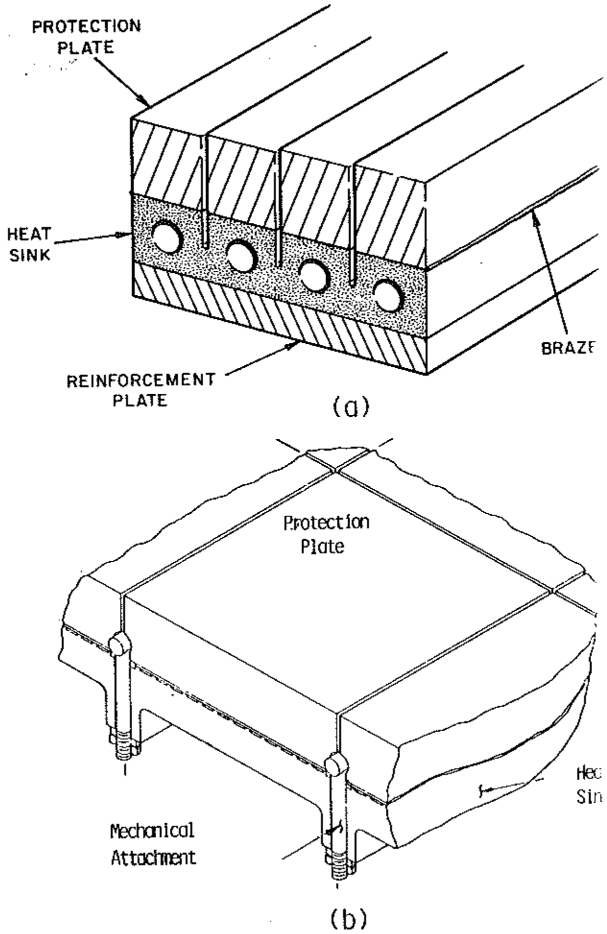

Fig. 3. Divertor collector plate designs: (a) h[illegible] conductance; and (b) low conductance.

The two designs result in considerably diff[illegible] operating conditions, as shown in Table 5. The [illegible] conductance concept has plate operating temperatu[illegible] 400-500°C compared with 2000-2300°C for the low c[illegible]tance concept. At the high operating temperature[illegible] the low conductance design, 40-50% of the inciden[illegible] is radiated back to the divertor chamber and the [illegible] chamber. The thermal radiation loss reduced the [illegible] gradient in the protection plate and the heat flu[illegible] the heat sink compared to the high conductance de[illegible] The high strength of the braze joint in the high [illegible]tance design results in high stresses at the bond [illegible]face due to the different rates of thermal expans[illegible] the protection plate and heat sink. The high st[illegible]

Table 5. Comparison of High Conductance and Low Conductance Design Concepts

	High Conductance	Low Conductance
Protection plate materials	W, ZM-6	W
Heat sink materials	Cu, Zircaloy	Austenitic stainless steel
Protection plate attachment	Braze	Mechanical
Typical plate temperatures	500°C	2200°C
Heat flux to heat sink	2.4 MW/m^2	1.1 MW/m^2
Mode of cooling	Thermal conduction	Radiation-thermal conduction
Primary concerns	Physical sputtering Braze integrity Thermal fatigue Radiation embrittlement	Physical sputtering Chemical sputtering Emissivity of sputtered W Embrittlement of recrystallized W

may produce fatigue crack growth and failure. The attachments in the low conductance design allow the protection plate to freely expand and rotate during the burn cycle, inducing very low stresses through the plate.

The primary materials issue for both designs is the high sputtering rate that will result in large material losses. Based upon available physical sputtering data and models, the high-Z elements are predicted to have the lowest sputtering rates for an incoming particle energy of ~400 eV. The sputtering analysis for INTOR has focused on the high-Z refractory metals such as molybdenum, tungsten, and their alloys. The physical sputtering rates of two materials, tungsten and ZM-6 (a molybdenum alloy), were analyzed during Phase-I. The self-sputtering has been taken into account. The effective sputtering coefficients are estimated to be 2.2×10^{-3} and 2.4×10^{-3} for tungsten and ZM-6, respectively. The resulting masterial loss rates are 5.22×10^{-10} m/s and 5.62×10^{-10} m/s, respectively. The estimated sputtering lifetime is 1.5-2 y at a 50% duty factor. There are uncertainties in the estimated sputtering coefficients.

The other materials issues for the high conductance design are shown in Table 5. Radiation embrittlement is expected to occur in the protection plate and heat sink materials. The ductile-brittle transition temperature of both molybdenum and tungsten have been observed to increase to 200-300°C after low temperature irradiation. Therefore the protection plate material must be treated as a brittle material for this design. Limited data indicate that radiation embrittlement could be severe in cold-worked copper.[6] However, since irradiation data does not exist for copper or copper alloys at high neutron fluence, there is a considerable uncertainty in the expected embrittlement for the operating conditions in INTOR. There is also a large uncertainty in the expected behavior of the braze bond. It is therefore not possible to evaluate the thermal fatigue lifetime, and additional experimental data are required for a complete evaluation.

The additional materials issues for the low conductance design are related to the high operating temperatures.[7] Chemical sputtering of tungsten, due to the presence of 0.5% oxygen in the plasma particle flux, may be significant. Chemical sputtering of tungsten is not well understood, however, and additional work is required. The surface temperature of tungsten depends upon the value of the emissivity. In order to achieve reasonable operating temperatures, the emissivity value should be greater than ~0.4, which requires a roughened surface. Sputtering is expected to influence the surface roughness, but the effect of sputtering on emissivity is not well characterized. If the emissivity values of a sputtered surface are low, then the operating temperatures will be excessive.

Acknowledgments

The author served as the USA INTOR Participant for Nuclear Systems. The work summarized in this paper is based on the effort of a large number of scientists and engineers in the USA, Europe, Japan, and USSR. The references listed below should be consulted for more technical details.

References

1. W. M. Stacey, Jr., "The INTOR Design - An Overview," these proceedings.
2. T. E. Shannon, "Engineering Features of the INTOR Conceptual Design," these proceedings.
3. J. A. Schmidt, "INTOR Physics," these proceedings.
4. INTOR - International Tokamak Reactor Phase-One Conceptual Design (IAEA, Vienna, 1981), to be issued.
5. "European Community Contribution to the International Tokamak Reactor Phase-I Workshop" (1981).
6. "Japan Contribution to the International Tokamak Rector Phase-I Workshop (1981).
7. "U.S. Contribution to the International Tokamak Reactor Phase-I Workshop" (1981).
8. "U.S.S.R. Contribution to the International Tokamak Reactor Phase-I Workshop" (1981).